ARTICLE NO. 79-4147

Aeroelastic Stability and Response of Horizontal Axis Wind Turbine Blades

S.B.R. Kottapalli* and P. P. Friedmann†
University of California, Los Angeles, Calif.
and
A. Rosen‡
Technion-Israel Institute of Technology, Haifa, Israel

Coupled flap-lag-torsion equations of motion of an isolated horizontal axis wind turbine (HAWT) blade have been formulated. The analysis neglects blade-tower coupling. The final nonlinear equations have periodic coefficients. A new and convenient method of generating an appropriate time-dependent equilibrium position, required for the stability analysis, has been implemented and found to be computationally efficient. Steady-state response and stability boundaries for an existing (typical) HAWT blade are presented. Such stability boundaries have never been published in the literature. The results show that the isolated blade under study is basically stable. The tower shadow (wake) has a considerable effect on the out-of-plane response but leaves blade stability unchanged. Nonlinear terms can significantly affect linearized stability boundaries; however, they have a negligible effect on response, thus implying that a time-dependent equilibrium position (or steady-state response), based completely on the linear system, is appropriate for the type of HAWT blades under study.

Nomenclature

A = blade cross-sectional area; also tower shadow parameter
$[A(\psi)]$ = periodic matrix
a = two-dimensional lift-curve slope
$B(\psi)$ = wind turbine tower wake (shadow) function
b = airfoil semichord
C_{do} = profile drag coefficient
E = Young's modulus
e_1 = offset of blade root from the axis of rotation
$\hat{e}_x,\hat{e}_y,\hat{e}_z$ = unit vectors in the directions of the coordinates x_0,y_0,z_0 before deformation
$\hat{e}'_x,\hat{e}'_y,\hat{e}'_z$ = the triad $\hat{e}_x,\hat{e}_y,\hat{e}_z$ after deformation
GJ = blade torsional rigidity
g = acceleration due to gravity
$g_i(\psi)$ = generalized coordinate for w
H = height of wind turbine tower
$h_i(\psi)$ = generalized coordinate for v
$[I]$ = identity matrix
I_2,I_3 = principal moments of inertia of cross section
$\boldsymbol{i},\boldsymbol{j},\boldsymbol{k}$ = unit vectors in the x,y,z directions
k_m = blade cross section mass radius of gyration
$[L(\psi)]$ = periodic matrix
ℓ = length of elastic part of blade
M_b = total blade mass
m = blade mass per unit length
$\{N(q,\psi)\}$ = vector containing nonlinear terms of q_i
$\bar{p}$ = distributed external force vector per unit length
$\bar{q}$ = distributed external moment vector per unit length
$\{q\}$ = state variable vector
$\{\bar{q}_L\}$ = vector defining the time-dependent equilibrium position
R = blade radius
$\boldsymbol{R}$ = position vector of a mass point on the elastic axis
t = time
$\bar{U}'$ = resultant nondimensional air speed
$\bar{U}'_T,\bar{U}'_p$ = resultant nondimensional velocity components in the $\hat{e}'_y,\hat{e}'_z$ directions
u,v,w = displacements of the elastic axis in the $\hat{e}_x,\hat{e}_y,\hat{e}_z$ directions
V_0 = gradient wind speed at $h=H$, $\bar{V}_0=V_0/(\Omega R)$
$\bar{V}_m$ = gradient wind speed
$\hat{X},\hat{Y},\hat{Z}$ = unit vectors in the x_1,y_1,z_1 directions
x,y,z = rotating coordinate system
$\bar{x}$ = x/ℓ
x_0,y_0,z_0 = initial coordinate system of the blade
x_1,y_1,z_1 = ground (and tower) fixed coordinate system
x_{II} = offset between elastic and tension centers
x_A ($\bar{x}_A=x_A/R$) = offset between aerodynamic and elastic centers
$\{Z(\psi)\}$ = periodic forcing vector
α = power law exponent
β_p = precone angle
γ = gradient wind inclination from $\hat{Z}$ axis
γ_a = $\rho aR^3/$(blade mass), nondimensional parameter
$\delta\bar{M}_y,\delta\bar{M}_z$ = cyclic components of steady-state bending moments $\bar{M}_y$ and $\bar{M}_z$; $\delta\bar{M}_y(0)$ and $\delta\bar{M}_z(0)$ denote values at blade root
ϵ = small parameter of the order of magnitude of the elastic slopes
ζ^i = real part of ith characteristic exponent; subscripts L and N refer to the linear and linearized systems, respectively

Received Sept. 20, 1978; revision received May 15, 1979.

Index categories: Aeroelasticity and Hydroelasticity; Wind Power; Propeller and Rotor Systems.

*Assistant Research Engineer, Mechanics and Structures Dept. Member AIAA.
†Associate Professor, Mechanics and Structures Dept. Associate Fellow AIAA.
‡Senior Lecturer, Dept. of Aeronautical Engineering.

$\theta_G(x_0)$ = total blade twist $[\theta_{GS}+\theta_{G0}(x_0)]$
$\theta_{G0}(x_0)$ = built-in twist
θ_{GS} = incremental collective pitch setting, "θ_G shift"
Λ_L^i = multiplier, eigenvalue of $[\Phi_L(2\pi)]$
ρ = air mass density
$[\Phi_L],[\Phi_N]$ = fundamental matrices
ϕ = rotation of a blade cross section about the elastic axis
ψ = azimuth angle, $=\Omega t$
$\Omega(\boldsymbol{\Omega}=\Omega k)$ = angular speed of rotation
$\bar{\omega}_{FI},\bar{\omega}_{LI},\bar{\omega}_{TI}$ = first rotating natural frequencies in flap, lag, torsion, respectively, nondimensionalized by Ω

Special Symbols

$(\,^*)$ = differentiation with respect to ψ
$(\,)_{,x}$ = differention with respect to x_0
$(\dot{})$ = differentiation with respect to t

Introduction

RECENT studies have indicated that wind energy has the potential to make a significant contribution toward supplying the energy requirements in regions where sufficiently strong winds exist. Large horizontal axis wind turbines in the 100-3000 kW range are currently being designed and tested as potential generators of electricity. The economic viability of this environmentally clean source of energy will be determined largely by the initial and operating costs of such machines. An economically viable wind turbine must be capable of operating for extended periods of time without requiring excessive maintenance and replacement of parts. Thus, the reduction of vibratory loads and stresses in the rotor, tower, power train, and control system is essential in order to avoid fatigue problems. Additionally, the rational design of wind turbines involves the establishment of the aeroelastic stability boundaries and the determination of the system response.

The literature on the structural dynamic and aeroelastic design of horizontal axis wind turbines is relatively new. Reference 1 is an excellent survey containing a qualitative discussion of the effects of size, number of blades, hub configuration, and type of control system on the turbine dynamic characteristics. In a second paper, Ormiston[2] considers the basic flapping response of a wind turbine blade using elementary analytical techniques and a simple, rigid, centrally-hinged, spring-restrained blade model.

Friedmann[3] has presented a detailed discussion of the problems associated with the aeroelastic modeling of large wind turbines. The single-blade problem was formulated and the coupled rotor-tower case briefly discussed. A more recent survey[4] on rotary wing aeroelasticity is of interest here. This survey covers helicopter applications only; however, the information presented is also useful for wind turbines.

Spera[5] has performed an approximate structural analysis for the DOE/NASA Mod-O wind turbine rotor. Kaza and Hammond[6] have considered the flap-lag stability of wind turbine rotors in the presence of velocity gradients using a simple, centrally-hinged model for the blade. Dugundji[7] has reviewed the whirl stability of a windmill on a flexible tower; experimental results on the vibrations of a small-scale wind tunnel model were also presented.

Reference 8 contains both a theoretical analysis of the coupled-rotor dynamics of an operating 100 kW wind turbine and a comparison with measurements. The analysis was performed by a modified version of the Rexor[9] rotorcraft simulation program and the results were compared with the measured response of the Mod-O wind turbine. Reasonable agreement was obtained. The computer program of Ref. 10 has the capability of analyzing the coupled rotor-tower dynamics of horizontal wind turbines. However, the limited amount of numerical results presented might indicate that the program has mainly a qualitative predictive capability.

Analytically, a single blade is the basic building block from which the rotor-tower model is constructed, and the analysis of an isolated rotor blade can be viewed as a prerequisite to the solution and understanding of the more complex rotor-tower system. Also, one of the main conclusions of a recent study[11,12] on the rotor-tower system is that the blade-tower coupling is relatively minor if the tower stiffness is high and the yaw mechanism dynamics are excluded from the analysis. A locked yaw drive (or a very stiff nacelle-tower connection) and a torsionally stiff tower result in insignificant yaw mechanism dynamics. Practically, the Mod-O configuration with a locked (or a very stiff) yaw drive corresponds to such a situation *and, consequently, the single-blade stability and response characteristics indeed are representative of the overall system*. The present study considers the aeroelastic stability and response of a horizontal axis wind turbine blade.

This paper has two main objectives. The first is the establishment of the aeroelastic stability boundaries for a horizontal axis wind turbine rotor blade and obtaining representative steady-state response solutions. Such stability boundaries have never been published in the literature. The second objective is to implement a new method for conveniently computing the periodic response of periodic systems.[13,14]

General Formulation

Basic Assumptions

A typical horizontal axis wind turbine configuration is shown in Fig. 1. The study assumes that:

1) The blade is cantilevered at the hub and its elastic axis is initially straight. Also, the feathering axis is preconed by a small angle β_p, and there exists an offset e_I between the blade root and the axis of rotation (Fig. 2). The blade can have built-in twist $\theta_{GO}(x)$ about the undeformed elastic axis and the total twist is:

$$\theta_G(x)=\theta_{GS}+\theta_{GO}(x)$$

(Fig. 3), where θ_{GS} is an incremental collective pitch setting at the hub, depending on the wind turbine operating condition.

2) The cross section is symmetric about the major principal axis and can have three distinct points, namely, the elastic, aerodynamic, and tension centers. The elastic and mass centers are coincident.

3) The blade material is isotropic and linearly elastic.

4) Plane cross sections that are normal to the elastic axis before deformation remain plane after deformation and normal to the deformed axis (Bernoulli-Euler hypothesis); the

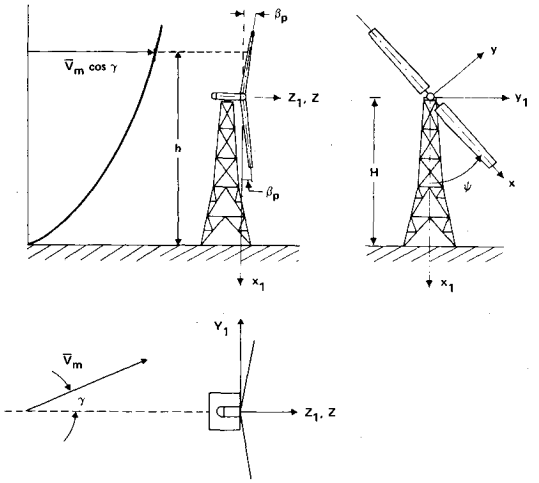

Fig. 1 Horizontal axis wind turbine configuration.

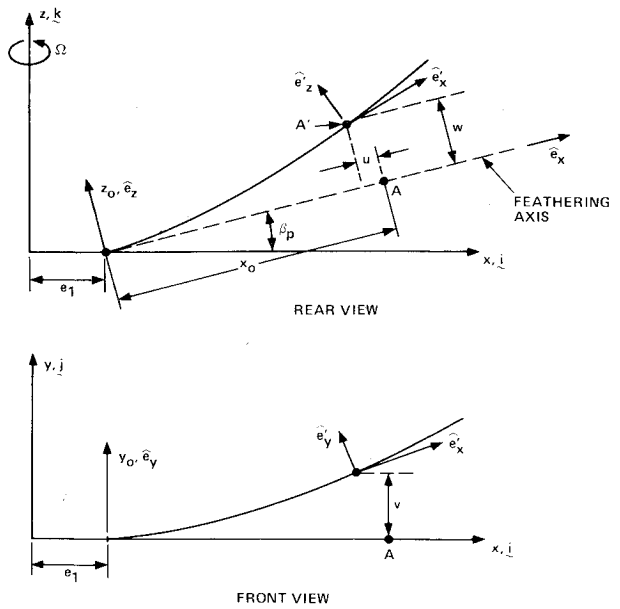

Fig. 2 Geometry of the elastic axis of deformed blade.

cross-sectional shape is unaffected by the deformations. Torsional warping is neglected.

5) The blade can bend in two mutually perpendicular directions normal to the elastic axis and has a distributed torsional rigidity, GJ.

6) The deflections, strains, and rotations (slopes) are small. Typical wind turbine blades are much stiffer than helicopter rotor blades. For example, the first flap, lag, and torsion natural frequencies of the Mod-O blade are, respectively, 3.3, 4.7, and 33.0 per revolution, as compared to 1.1, 1.4, and 5.0 for a typical helicopter rotor blade. Thus, wind turbine blades of the Mod-O type are at least an order of magnitude stiffer than helicopter blades; consequently, the wind turbine blade elastic deformations are significantly smaller than those of a helicopter blade. Therefore, the nonlinear structural terms are much less important for wind turbines. In addition, note that the wind turbine torsion frequency is an order of magnitude greater than its bending frequencies. This implies that the effect of the nonlinear bending-torsion coupling terms in the structural operator (Mil'-type terms[15]) would be small and unimportant for sufficiently small values of the precone.[15] Consequently, these nonlinear elastic terms are not retained in the equations.

7) The angular speed of the blade Ω is constant.

8) Quasisteady blade element strip theory is applicable, and apparent mass effects are negligible.

9) There is no blade-tower coupling. This is a valid assumption when the tower stiffness is high and yaw mechanism dynamics can be excluded from the analysis.[11,12] The Mod-O configuration with a locked or very stiff yaw drive represents a real case when this assumption is valid. Additional assumptions are noted in the text.

Ordering Scheme

An essential feature of the analysis is the introduction of a small parameter ϵ of the order of the elastic slopes.[4] The assigned orders of magnitudes of the important quantities are:

$$x/\ell,\ \partial(\ )/\partial\psi,\ \partial(\ )/\partial\bar{x} \sim O(1)$$

$$\bar{V}_0,\ \theta_G \sim O(\epsilon^{1/2})$$

$$\partial w/\partial x,\ \partial v/\partial x,\ \phi,\ \beta_p,\ b/R,\ e_1/\ell \sim O(\epsilon)$$

$$x_A/R \sim O(\epsilon^{1.5})$$

$$u/\ell,\ C_{do}/a,\ k_m^2/\ell^2 \sim O(\epsilon^2)$$

The present ordering scheme is slightly different from those usually employed in helicopter rotor blade analyses. For example, the mean wind velocity $\bar{V}_0$, which provides a major contribution to the total inflow through the rotor is assigned an order of magnitude $\epsilon^{1/2}$ (instead of ϵ for the corresponding inflow of a helicopter rotor). This is done to account for the operating conditions of some existing designs (Mod-O). It is emphasized that the ordering scheme is not adhered to rigidly. Certain terms which are apparently negligible within the context of the scheme are nevertheless retained. The drag damping term in the lag equation is one example. In general, within any equation, terms of order higher than ϵ^2 are dropped, i.e., terms of order $\epsilon^{2.5}$, ϵ^3, or higher, are neglected.

Basic Equations of Motion

The equations of motion are taken from Refs. 16 and 17, where only the structural operator is expressed explicitly,

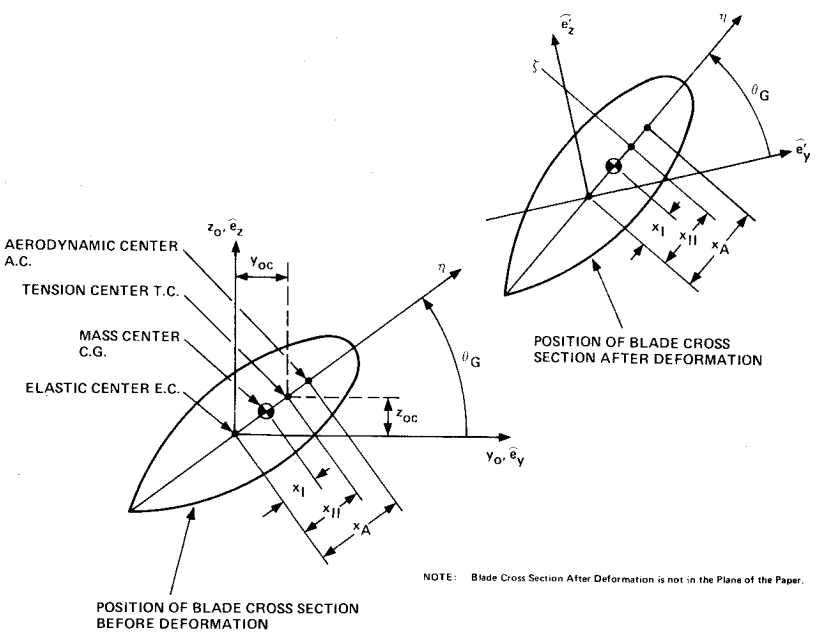

Fig. 3 Blade cross section positions before and after deformation.

while all other contributions are represented symbolically. In view of assumption 6, the equations employed in this study are equivalent to those of Houbolt and Brooks[18] in the sense that both essentially represent a linear treatment of the structural operator. Note that the pretwist term, present in the torsion equation of Ref. 18, is absent in the equations of Ref. 16 (and of this study). According to Ref. 18, the effect of pretwist is to slightly increase the torsional stiffness. Considering the very high torsional stiffness of the wind turbine blades under study in this paper, a small change in this high stiffness cannot have any significant effect on the present results. Furthermore, it should be noted that the exact treatment of pretwist requires the combined use of curvilinear coordinates and warping.[19,20]

Expressed in the undeformed coordinate system, the coupled equilibrium equations (Eq. (32) of Ref. 16) for the axial, lag, flap, and torsion degrees of freedom are:

$$T_{,x}+(\tilde{q}_z v_{,x})_{,x}-(\tilde{q}_y w_{,x})_{,x}+\tilde{p}_x=0 \tag{1}$$

$$[(EI_2\cos^2\theta_G+EI_3\sin^2\theta_G)v_{,xx}+(EI_2-EI_3)\times\sin\theta_G\cos\theta_G w_{,xx}-Tx_{II}\cos\theta_G]_{,xx}-(Tv_{,x})_{,x}+\tilde{q}_{z,x}-(w_{,x}\tilde{q}_x)_{,x}-\tilde{p}_y=0 \tag{2}$$

$$[(EI_2-EI_3)\sin\theta_G\cos\theta_G v_{,xx}+(EI_2\sin^2\theta_G+EI_3\times\cos^2\theta_G)w_{,xx}-Tx_{II}\sin\theta_G]_{,xx}-(Tw_{,x})_{,x}-\tilde{q}_{y,x}+(v_{,x}\tilde{q}_x)_{,x}-\tilde{p}_z=0 \tag{3}$$

$$(GJ\phi_{,x})_{,x}+\tilde{q}_z w_{,x}+\tilde{q}_y v_{,x}+\tilde{q}_x=0 \tag{4}$$

where the tension is given by

$$T=EA[u_{,x}+\tfrac{1}{2}(v_{,x}^2+w_{,x}^2)-x_{II}\cos\theta_G v_{,xx}-x_{II}\sin\theta_G w_{,xx}] \tag{5}$$

The distributed load vectors are expressed as:

$$\tilde{p}=\tilde{p}_x\hat{e}_x+\tilde{p}_y\hat{e}_y+\tilde{p}_z\hat{e}_z=\tilde{p}_I+\tilde{p}_A+\tilde{p}_g+\tilde{p}_s \tag{6}$$

$$\tilde{q}=\tilde{q}_x\hat{e}_x+\tilde{q}_y\hat{e}_y+\tilde{q}_z\hat{e}_z=\tilde{q}_I+\tilde{q}_A+\tilde{q}_g+\tilde{q}_s \tag{7}$$

where the subscripts I, A, g, and s refer to the inertial, aerodynamic, gravitational, and structural damping contributions, respectively.

Formulation of the Loads

Details about the following are given in Ref. 14. In the rotating (x,y,z) frame, the position vector of a mass point on the elastic axis is:

$$R=e_1 i+(x_0+u)\hat{e}_x+v\hat{e}_y+w\hat{e}_z \tag{8}$$

The coordinate systems are shown in Figs. 1-3 and the transformations between them are given in Ref. 14. A linear transformation matrix is used to relate the deformed and undeformed elastic axis positions. Such a representation is quite appropriate for the relatively stiff blades of wind turbines under study. Also, it is straightforward to show that using a linear transformation is consistent with respect to the ordering scheme and that all nonnegligible terms are included in the equations. The blade velocity and acceleration are (Ref. 21, pp. 264-270):

$$V_B=\dot{R}+(\Omega\times R) \tag{9}$$

$$a=\ddot{R}+(2\Omega\times\dot{R})+\Omega\times(\Omega\times R) \tag{10}$$

From D'Alembert's principle, the inertia force distribution is:

$$\tilde{p}_I=-ma=\tilde{p}_{xI}\hat{e}_x+\tilde{p}_{yI}\hat{e}_y+\tilde{p}_{zI}\hat{e}_z \tag{11}$$

and within the assumptions of the analysis, the inertia moment distribution is:

$$\tilde{q}_I=\tilde{q}_{xI}\hat{e}_x \tag{12}$$

where the final expressions for $\tilde{q}_I$ were obtained by assuming that the blade mass is compressed into an infinitesimally thin plate.

Aerodynamic Loads

Aerodynamic forces and moments are obtained from quasisteady blade element strip theory. Contributions from atmospheric winds, blade velocity [Eq. (9)], induced velocity, and tower shadow effects are included.

Atmospheric winds are taken to be the gradient mean wind and superimposed simple harmonic gust components.[3] The gradient mean wind is represented by a boundary-layer power law profile

$$\bar{V}_m/\bar{V}_0=(h/H)^{\alpha} \qquad 0.15\le\alpha\le 0.45 \tag{13}$$

where the height of the elastic center is (Fig. 1):

$$h=H-(e_1+x_0)\cos\psi$$

To facilitate the solution procedure, the power law profile is replaced by its Taylor series expansion about $h=H$. Only the first three terms of the series are retained. The total atmospheric wind velocity is:

$$V_A=V_m+V_g \tag{14}$$

where V_m is the vector representation of $\bar{V}_m$, and V_g is the gust contribution.

For downwind rotors, the tower wake (shadow) has a significant effect on blade dynamics.[22,23] This effect is included by introducing a blockage factor, $B(\psi)\le 1$, such that the gradient wind for ψ inside the shadow, say, $\psi_2\le\psi\le\psi_1$, is $(B\bar{V}_m)$, and for all other locations, the mean wind is simply $\bar{V}_m$. The limits ψ_1 and ψ_2, and the function $B(\psi)$, empirically specified, are based on wind-tunnel data and full-scale wake measurements. The particular wake function employed is given in the section on results.

The total velocities are:

$$\bar{U}_T'=[(V_A-V_B)_T]/(\Omega R) \tag{15}$$

$$\bar{U}_P'=[(V_A-V_B)_P+\nu]/(\Omega R) \tag{16}$$

where the subscripts T and P refer to the directions $\hat{e}_y'$ and $\hat{e}_z'$, respectively, and ν is the induced velocity.[14]

From blade element theory, the drag acts in the direction of the resultant velocity $\bar{U}'$, and the lift perpendicular to it. The elemental lift and drag magnitudes per unit length are:

$$L=\rho ab(\Omega R)^2(\bar{U}')^2\alpha_e \tag{17}$$

$$D=\rho b(\Omega R)^2(\bar{U}')^2 C_{do} \tag{18}$$

where

$$\bar{U}' = [(\bar{U}_T')^2 + (\bar{U}_p')^2]^{1/2} \tag{19}$$

$$\alpha_e = \theta_G + \phi_i$$

$$\sin\phi_i = \bar{U}_p'/\bar{U}'$$

$$\cos\phi_i = -\bar{U}_T'/\bar{U}'$$

For wind turbines it is not necessary that the inflow angle ϕ_i be small; however, for unstalled conditions, the effective angle of attack α_e can be assumed small, thus allowing α_e to be approximated by $\sin\alpha_e$. The *aerodynamic force* distribution is then

$$\bar{p}_A = \boldsymbol{L} + \boldsymbol{D} = \bar{p}_{xA}\hat{e}_x + \bar{p}_{yA}\hat{e}_y + \bar{p}_{zA}\hat{e}_z \tag{20}$$

where $\boldsymbol{L}$ and $\boldsymbol{D}$ are vector representations of L and D. The *aerodynamic moment* distribution is simply

$$\bar{q}_A = x_A L\cos\alpha_e \hat{e}_x' \tag{21}$$

where the negligible drag contribution has been dropped.

Equations (20) and (21) contain several negligible terms. In the final equations, the drag contribution is retained only in the lag force $\bar{p}_{yA}$. When the expressions for $\bar{U}_T'$, $\bar{U}_P'$, and $\bar{U}'$ are substituted, a considerable number of terms are found to be negligible within the ordering scheme and are not retained. Also, all nonlinear terms involving the torsional deformation ϕ are dropped. This is justified by the relatively high torsional rigidity of the configurations under study. It is emphasized that nonlinear terms involving the bending displacements/slopes are retained. Overall, it should be recognized that this is inconsistent with respect to the ordering scheme. Such a procedure implies that the torsional deformation ϕ has been implicitly treated to be of an order higher than ϵ, i.e., $\epsilon^{1.5}$ or even ϵ^2. Of course, physically, this procedure is quite realistic since the blade is much stiffer in torsion as compared to bending.

Considered next is the resultant air speed, present in the drag term of $\bar{p}_{yA}$ and defined by Eq. (19) as

$$\bar{U}' = (\bar{U}_T'^2 + \bar{U}_P'^2)^{1/2}$$

The expressions for $\bar{U}_T'$ and $\bar{U}_P'$ contain the unknown elastic displacements/deformations and the square root operator involving these variables is inconvenient to use. The preceding equation can be expressed as

$$\bar{U}' = [1 + (\bar{U}_P'/\bar{U}_T')^2]^{1/2}\,|\bar{U}_T'|, \qquad \bar{U}_T' \neq 0$$

In helicopter rotor analysis it is common to replace $\bar{U}'$ by $|\bar{U}_T'|$, since for these applications $(\bar{U}_P'/\bar{U}_T')^2 \sim 0(\epsilon^2) \ll 1$. For wind turbines, however, the relatively high inflow $(\bar{U}_P'/\bar{U}_T')^2 \sim 0(\epsilon)$ precludes such an approximation. For the drag term in $\bar{p}_{yA}$, the present study approximates the resultant air speed by

$$\bar{U}' = f_2\,|\bar{U}_T'|$$

where f_2 is obtained by evaluating $[1 + (\bar{U}_P'/\bar{U}_T')^2]^{1/2}$ for the case of a *rigid rotor*. Note that f_2 (≥ 1) is a function of x_0 and ψ.

Gravity force is simply $\bar{p}_g = mg\hat{X}$ and coincident mass and elastic centers imply that $\bar{q}_g = 0$. Structural damping loads are assumed to be of a viscous type.[3,14]

The various loads are assembled in Eqs. (1-7), and the assumption of a very high radial stiffness (equivalent to axial inextensibility) facilitates the elimination of the axial displacement u and the tension T from Eqs. (2-4). This results in three coupled, nonlinear, second-order, partial-differential equations for the variables v, w, and ϕ.[14]

Solution Procedure

The elastic degrees of freedom are represented by the uncoupled free-vibration modes of a nonuniform rotating blade

$$w = \ell\eta_i(x_0)\,g_i(\psi)$$

$$v = -\ell\gamma_i(x_0)\,h_i(\psi)$$

$$\phi = \phi_j(x_0)\,f_j(\psi) \tag{22}$$

where repeated indices imply summation and $i,j = 1,2,\ldots,N$. Application of Galerkin's method eliminates the spatial dependency, resulting in a system of $3N$ nonlinear, second-order, ordinary-differential equations which is subsequently converted to the following nonlinear first-order system with $6N$ equations

$$\{\dot{q}\} = \{Z(\psi)\} + [L(\psi)]\{q\} + \{N(q,\psi)\} \tag{23}$$

where the new vector $\{q\}$ represents the state variables, $\{Z(\psi)\}$ and $[L(\psi)]$ are independent of the q_i's, $i = 1,\ldots,6N$, and $\{N(q,\psi)\}$ contains the nonlinear terms. In the present case of periodic excitation

$$\{Z(\psi)\} = \{Z(\psi + 2\pi)\} \text{ and } [L(\psi)] = [L(\psi + 2\pi)] \tag{24}$$

Time-Dependent Equilibrium Position

Stability boundaries can be obtained by first computing an appropriate equilibrium position and then examining the behavior of small perturbations about this position. For a linear stability analysis, an equilibrium position is "appropriate" if the perturbations about this position are sufficiently small, such that nonlinear perturbation terms are negligible. Previous analyses (for example, Ref. 24) have used a relatively simple version of the harmonic balance technique to find an equilibrium position. However, this approach is algebraically tedious and, in practice, it is rare that harmonics higher than the first are retained in the equations. Depending on the periodic excitation, such a simplification can seriously limit the accuracy and reliability of the final results. There is a second drawback which is noted later in this section.

The present study does not use the harmonic balance method. Instead, certain properties of linear systems with periodic coefficients are utilized to generate a time-dependent (periodic) equilibrium position. Consider the following linear version of the nonlinear system, Eq. (23),

$$\{\dot{q}_L\} = \{Z(\psi)\} + [L(\psi)]\{q_L\} \tag{25}$$

where $\{q_L\}$ satisfies Eq. (25). Periodic solutions of this linear system (with periodic coefficients) are of interest here; let $\{\bar{q}_L\}$ be such a solution, i.e., $\{\bar{q}_L(\psi)\} = \{\bar{q}_L(\psi + 2\pi)\}$.

Urabe[25] has shown that if the multipliers of the corresponding homogeneous system

$$\{\dot{q}_H\} = [L(\psi)]\{q_H\} \tag{26}$$

are all different from one, then Eq. (25) has one and only one periodic solution of period 2π, which is exactly given by

$$\{\bar{q}_L\} = [\Phi_L(\psi)]\left\langle \int_0^{\psi} [\Phi_L(s)]^{-1}\{Z(s)\}\,ds + ([I] - [\Phi_L(2\pi)])^{-1}[\Phi_L(2\pi)]\cdot\int_0^{2\pi} [\Phi_L(s)]^{-1}\{Z(s)\}\,ds \right\rangle \tag{27}$$

where $[I]$ is the identity matrix and $[\Phi_L]$ the fundamental matrix of Eq. (26) defined by

$$\left.\begin{aligned} [\dot{\Phi}_L(\psi)] &= [L(\psi)][\Phi_L(\psi)] \\ [\Phi_L(0)] &= [I] \end{aligned}\right\} \tag{28}$$

Note that the condition for the existence of a unique periodic solution of Eq. (25) is that the determinant of $([I] - [\Phi_L(2\pi)])$ be nonzero. This is satisfied if all the multipliers of Eq. (26), the Λ_L^i's, are different from unity, which is equivalent to the condition that the real parts of all characteristic exponents be nonzero, i.e., $\zeta_L^i \neq 0$. From Floquet theory (Ref. 21, p. 264), if all the $\zeta_L^i < 0$, then the homogeneous system is asymptotically stable; if any one $\zeta_L^i > 0$, the homogeneous system becomes asymptotically unstable. In the former case, Eq. (27) is the steady-state solution of the linear system, Eq. (25). When any one $\zeta_L^i > 0$, the mathematical expression for $\{\bar{q}_L\}$ is still valid; however, the periodic solution of Eq. (25) is of no practical significance. Hsu and Cheng[26] have made some interesting comments in this regard. Obviously the (approximate) time-dependent equilibrium position used in the stability analysis should be physically meaningful. If Eq. (27) is employed as an approximate equilibrium position for the nonlinear system, then a check must be made as to whether or not the linear system is asymptotically stable. In the harmonic balance technique there is no simple way of obtaining such information.

In the present study, determination of the time-dependent equilibrium position is based on Eq. (27) instead of a more exact solution to the full nonlinear Eq. (23). Whereas this may or may not be justifiable for the relatively flexible helicopter blades, at least for the much stiffer wind turbine blades it is expected that nonlinear terms would have an insignificant effect on response, i.e., the equilibrium position. This assumption is completely validated by the numerical response results presented later. Recognizing that Eq. (27) is a special case of the general solution of Eq. (25) with the following initial condition

$$\{q_L(0)\} = ([I] - [\Phi_L(2\pi)])^{-1}[\Phi_L(2\pi)] \times \int_0^{2\pi} [\Phi_L(s)]^{-1}\{Z(s)\}ds \tag{29}$$

the periodic solution $\{\bar{q}_L\}$ is obtained by numerically integrating Eq. (25) with the preceding initial condition.

Stability Analysis and Steady-State Response

Consider the original nonlinear equation, Eq. (23). Linearizing this equation about the time-dependent equilibrium position yields the homogeneous part of the perturbation equation as

$$\{\Delta\dot{q}^*\} = [A(\psi)]\{\Delta q\} \tag{30}$$

where

$$\{q(\psi)\} = \{\bar{q}_L(\psi)\} + \{\Delta q(\psi)\} \tag{31}$$

$$[A(\psi)] = [L(\psi)] + [\partial N/\partial q(\bar{q}_L, \psi)] \tag{32}$$

and

$$[A(\psi)] = [A(\psi + 2\pi)] \tag{33}$$

The second term of $[A(\psi)]$ is the Jacobi matrix of $\{N(q,\psi)\}$.

The linearized system is asymptotically stable if all $\zeta_N^i < 0$, where ζ_N^i are the real parts of the characteristic exponents associated with $[\Phi_N(\psi)]$ which is defined by

$$[\dot{\Phi}_N^*(\psi)] = [A(\psi)][\Phi_N(\psi)], \quad [\Phi_N(0)] = [I] \tag{34}$$

Theoretical details on the preceding and the efficient computation of transition matrices are given in Ref. 27.

As noted earlier, the equilibrium position employed in this study is the same as the steady-state response of the linear system, Eq. (25). For present purposes this solution is presumed to represent the nonlinear steady-state response with sufficient accuracy. This presumption, that in the present case nonlinear terms would have an insignificant effect on blade response, is completely validated by the numerical results on response presented in the next section.

Results

The numerical results presented here are based on the following simplifying assumption. One uncoupled rotating mode shape at zero twist setting was used to represent each elastic degree of freedom, i.e., $N=1$ in Eq. (22). The basic configuration studied was the Mod-O blade which has nonuniform sectional properties.[22,28] The calculated frequencies were $\bar{\omega}_{FI} = 2.89$, $\bar{\omega}_{LI} = 4.36$, and $\bar{\omega}_{TI} = 29.61$. The following were also kept constant in the computations: $R = 19.0$ m; $e_1/\ell = 0.068$; $\ell/R = 0.936$; $\ell/H = 0.585$; $k_m/\ell = 0.020$; $C_{do} = 0.01$; $a = 2\pi$; $\alpha = 0.15$; $x_{II} = 0.0$; $\gamma_a = 58.7$; $g/(\Omega^2\ell) = 0.0313$; $M_b = 907$ kg; and $\Omega = 4\pi/3$ rad s^{-1}. All structural damping coefficients and gust magnitudes were set to zero. Other parameters are specified on the plots.

Typical CPU time per run (both stability and response information) was 10 s on the IBM 360/91. Thus, the new procedure for obtaining the time-dependent equilibrium position is both convenient and computationally very efficient.

The two blades of the Mod-O configuration are designed to produce 133 kW of shaft power, the resulting electrical output being 100 kW. The θ_{GS} required to maintain a *constant power output (trim)* was obtained by considering quasisteady aerodynamics of a rigid blade.[14] Shown in Fig. 4 is the resulting trim curve for a perfectly aligned rotor ($\gamma = 0$ deg). Note that at $\bar{V}_0 = 0.10$, $\theta_{GS} = 0$ deg.

Stability

Recall that the ζ_N^i's refer to the linearized version of the nonlinear system, Eq. (30), and the ζ_L^i's represent the homogeneous part of the linear system, Eq. (26), in which all nonlinear terms have been dropped. In the stability plots, results obtained from the linearized system are referred to as "nonlinear," and those from the linear system are termed as "linear."

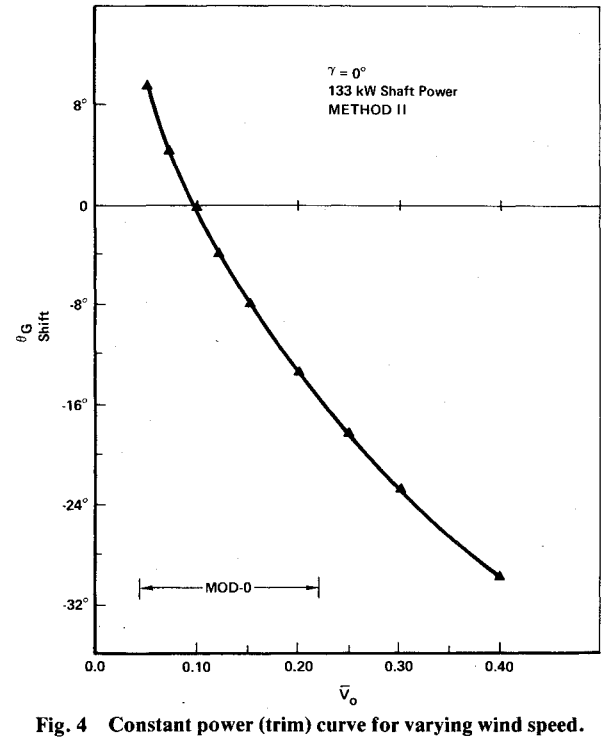

Fig. 4 Constant power (trim) curve for varying wind speed.

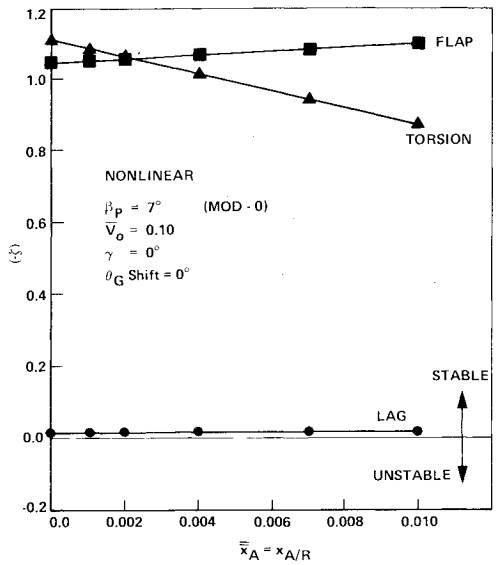

Fig. 5 Effect of aerodynamic offset on blade stability (trimmed).

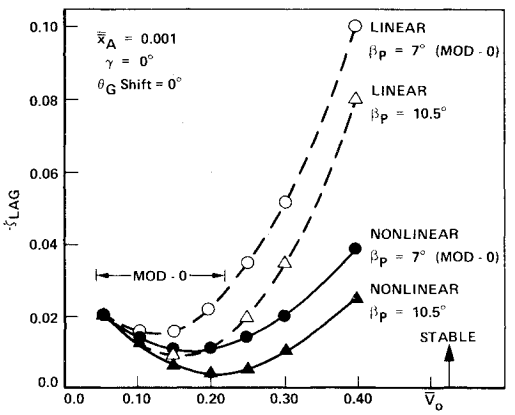

Fig. 6 Lag stability, effect of mean wind and precone, $\theta_{GS} = 0$ deg (untrimmed).

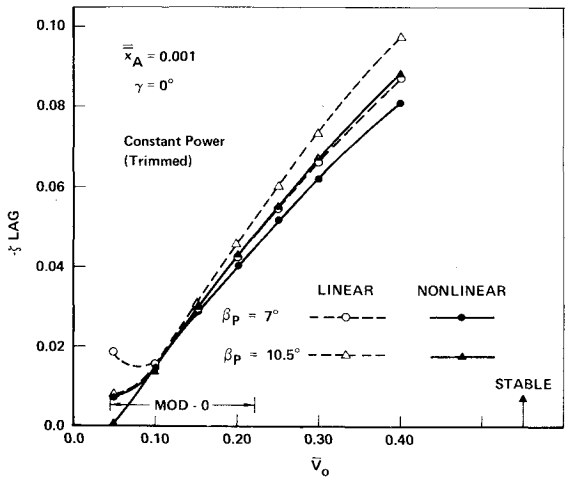

Fig. 7 Lag stability, effect of mean wind and precone, constant power (trimmed).

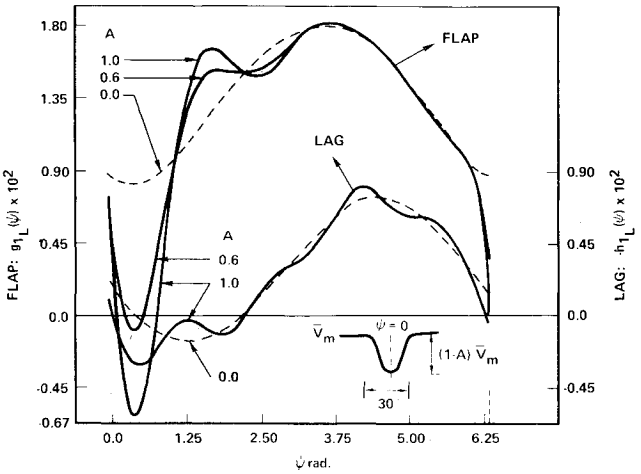

Fig. 8 Tower shadow effect on steady-state response, $\beta_p = 7$ deg, $\bar{x}_A = 0.001$, $\bar{V}_0 = 0.10$, $\gamma = 0$ deg, θ_G shift = 0 deg, $W = 30$ deg.

Figure 5 illustrates the relative stability characteristics of the three degrees of freedom shown for several values of the aerodynamic offset. Clearly, it is the lag degree of freedom which is potentially unstable. This is characteristic of hingeless configurations and also justifies the careful handling of higher-order lag-damping terms. Finally, lag stability is practically insensitive to variations in the aerodynamic offset.

For all the cases considered in this study, the ζ's for the flap and torsion degrees of freedom stayed close to minus one, indicating that these are very stable. Consequently, the following figures contain variations of ζ for the lag degree of freedom only.

Figure 6 (untrimmed case) shows that in the operating range of the Mod-O the blade is stable. Further, near the lower end of this range the linear and linearized results are essentially the same. At higher wind speeds, however, the linear results deviate considerably from the linearized ones. Clearly, the nonlinearities have a destabilizing effect on the blade. That an increase in the precone is always destabilizing for this condition is also evident.

The more practical constant power (trimmed) results of Fig. 7 contradict some of the preceding trends; however, the basic conclusion that the blade is stable is left unchanged. Recall that at wind speeds greater than $\bar{V}_0 = 0.10$, a negative θ_{GS} is required to maintain constant power, and for $\bar{V}_0 < 0.10$, a positive θ_{GS} is needed (Fig. 4). That blade stability is directly affected by this operational feature is evident from Fig. 7 where, compared to the $\theta_{GS} = 0$ deg case, for $\bar{V}_0 > 0.10$, the blade is more stable and the (destabilizing) effect of the nonlinearities is smaller; for $\bar{V}_0 < 0.10$, the trend is the opposite, i.e., the constant power blade is less stable and the destabilizing effect of the nonlinearities has increased. At higher wind speeds, the basic behavior is the same, namely, the linear results deviate from the linearized ones. Finally, an increase in precone is stabilizing for $\bar{V}_0 > 0.10$ and destabilizing for $\bar{V}_0 < 0.10$.

To summarize, the constant power (trimmed) blade is generally more stable than the untrimmed one. Both operating conditions result in a basically stable blade. Also, introduction of the constant power condition reduces, in general, the importance of nonlinear effects. Depending on the operating condition, precone can be either stabilizing or destabilizing. The nonlinear contributions were always destabilizing for the cases considered.

It was found that the tower shadow has an insignificant effect on blade stability. Several cases were investigated: $0.05 \leq \bar{V}_0 \leq 0.40$, $\theta_{GS} = 0$ deg, and constant power condition, all with $\gamma = 0$ deg. The blockage factor was specified for -15 deg $< \psi < 15$ deg as

$$B(\psi) = 1 - (A/2)[1 + \cos(12\psi)] \tag{35}$$

and $B(\psi) = 1$ for ψ outside the 30-deg sector. The wind speed decrement amplitude A varied from 0.0 to 1.0, and the resulting maximum change in the ζ for lag was 4.5%.

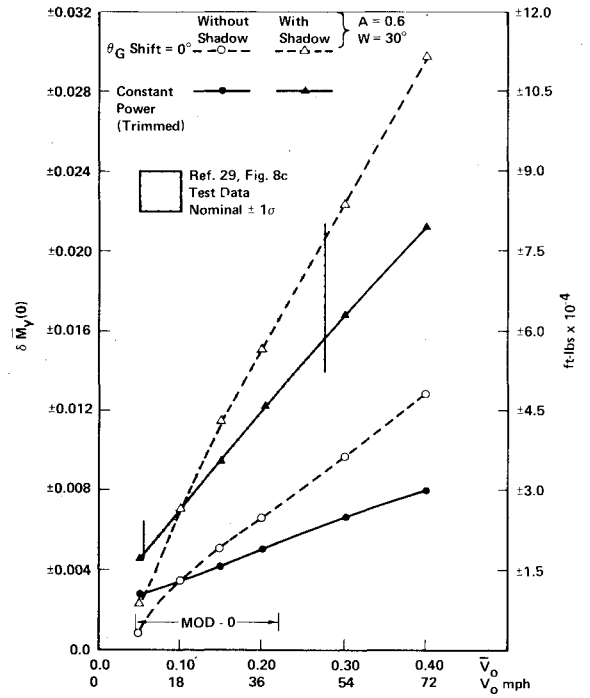

Fig. 9 Out-of-plane cyclic moment variation with mean wind, $\gamma = 0$ deg.

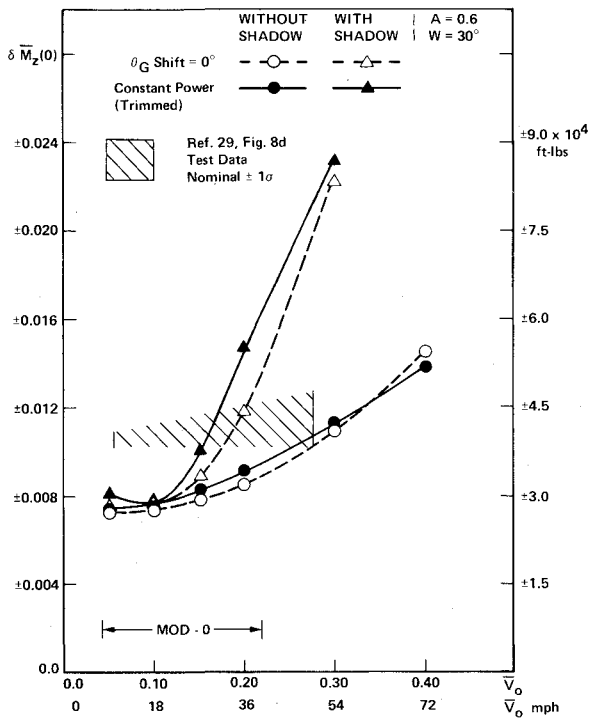

Fig. 10 In-plane cyclic moment variation with mean wind, $\gamma = 0$ deg.

Steady-State Response

Recall that the present formulation for obtaining the steady-state response of the linear system is exact. The numerical results of this study are based on a one-mode representation for each elastic degree of freedom.

Figure 8 shows typical flap and lag steady-state responses based on Eq. (27). The corresponding displacements are given by $w = \ell \eta_1(\bar{x}_0) g_{1L}(\psi)$ and $v = -\ell \gamma_1(\bar{x}_0) h_{1L}(\psi)$ where $\eta_1(1) = \gamma_1(1) = 1$. Comparatively, the torsional response was ten times smaller and is not shown. That the flap response is more sensitive to the tower shadow is evident from the figure, in which the shadow parameter A varies from 0.0 to 1.0. The qualitative behaviors of the responses are remarkably similar to the measured bending moments given in Refs. 23 and 29, thus reinforcing the presumption that a single-mode representation is adequate for a trend-type study such as the present one.

Consider the steady-state root bending moments which are of practical interest. The data are presented as cyclic components defined by $\delta \bar{M}_y = (1/2)(\bar{M}_{y,\max} - \bar{M}_{y,\min})$ and $\delta \bar{M}_z = (1/2)(\bar{M}_{z,\max} - \bar{M}_{z,\min})$ where the subscripts y and z stand for the out-of-plane and in-plane components, respectively. The moments are nondimensionalized by $(M_b \Omega \ell^2)$, and the basic bending moment-curvature relations were used to compute the cyclic components. It is cautioned that, first, a one-mode representation is usually inadequate for accurate predictions of the root moments and second, the use of the moment-curvature expressions to directly compute the moments can lead to highly erroneous quantitative results. In principle, a more sophisticated method, such as the "mode acceleration," could be implemented. For the present trend-type study, this was deemed unnecessary. Shown in Figs. 9 and 10 is the increase in cyclic moments due to an increase in mean wind speed. Both the tower shadow and mode of operation significantly affect the cyclic components. Compared to the $\theta_{GS} = 0$ deg condition, the constant power operation generally results in a smaller out-of-plane cyclic moment (Fig. 9). The trend for the in-plane cyclic moment is not so clearly defined. Also shown in Figs. 9 and 10 are the test data for the Mod-O with locked yaw drive taken from Figs. 8c and 8d of Ref. 29. The agreement between the measured data band and the present constant power (100 kW) with tower shadow out-of-plane cyclic moment is quite good, Fig. 9. However, the corresponding in-plane component does not compare so well. Overall, the results demonstrate that the essential qualitative and out-of-plane quantitative features can be recovered by a one-mode representation.

Finally, the *effect of nonlinearities on blade response is considered.* This was investigated by numerically integrating the nonlinear equation, Eq. (23), with the initial condition, Eq. (29), corresponding to the linear system given by Eq. (25). Recall that this initial condition guarantees a periodic (steady-state) response for the linear system only, and its use with the nonlinear equation will result in a transient response. The difference between this transient output and the steady-state response of the linear system should give an idea about the effect of nonlinearities on blade response. Several cases were investigated: $0.05 \le \bar{V}_0 \le 0.40$ with $\gamma = 0$ deg, $\theta_{GS} = 0$ deg, $\beta_p = 7$ deg, $\bar{x}_A = 0.001$, and the integration was carried out to four blade revolutions. It was found that the respective blade root moments differed by less than 5%, implying that nonlinear terms have a very small effect on blade response. This validates the earlier assumption that a time-dependent equilibrium position/steady-state response based on the linear system, Eq. (25), is quite appropriate for the type of wind turbine blades under study.

Conclusions

A formulation of the equations of motion governing the flap-lag-torsional dynamics of an isolated wind turbine blade has been presented. These equations were employed to obtain the aeroelastic stability and response of a large horizontal axis wind turbine blade. Such stability boundaries have never been published in literature. Futhermore, a new and convenient method of generating an appropriate time-dependent equilibrium position has been implemented and found to be computationally efficient.

The results presented are mainly applicable to an existing blade design (DOE/NASA Mod-O) and should be considered indicative of trends due to the assumptions used. The major conclusions are:

1) The Mod-O configuration is a basically stable design.

2) Both blade stability and response are sensitive to the mode of operation.

3) Blade stability can be sensitive to the precone angle depending on the mode of operation. Only the average out-of-plane response is significantly affected by variations in precone.[14]

4) The tower shadow (wake) has a considerable effect on the out-of-plane response, but leaves blade stability unchanged.

5) Nonlinear terms can significantly affect the linearized stability boundaries; however, they have a negligible effect on blade response, thus implying that a time-dependent equilibrium position or steady-state response completely based on the linear system (as in the present study) is appropriate for the type of blades under consideration.

Acknowledgment

This research was supported by NASA Lewis Research Center, Cleveland, Ohio under NASA Grant NSG 3082.

References

[1] Ormiston, R. A., "Rotor Dynamic Considerations for Large Wind Power Generator Systems," *Proceedings of the Wind Energy Conversion Systems Workshop*, National Science Foundation, NSF/RA/W-73-006, Dec. 1973.

[2] Ormiston, R. A., "Dynamic Response of Wind Turbine Rotor Systems," AHS Preprint S-993, presented at the Thirty-First Annual National Forum of the American Helicopter Society, Washington, D.C., May 1975.

[3] Friedmann, P. P., "Aeroelastic Modeling of Large Wind Turbines," *Journal of the American Helicopter Society*, Vol. 21, No. 4, Oct. 1976, pp. 17-27.

[4] Friedmann, P. P., "Recent Developments in Rotary-Wing Aeroelasticity," *Journal of Aircraft*, Vol. 14, Nov. 1977, pp. 1027-1041.

[5] Spera, D. A., "Structural Analysis of Wind Turbine Rotors for the NSF-NASA MOD-O Wind Power System," NASA TM X-3198, March 1975.

[6] Kaza, K.R.V. and Hammond, C. E., "Investigation of Flap-Lag Stability of Wind Turbine Rotors in the Presence of Velocity Gradients and Helicopters in Forward Flight," *Proceedings, Seventeenth Structures, Structural Dynamics, and Materials Conference, AIAA/ASME/SAE*, King of Prussia, Pa., May 1976, pp. 421-431.

[7] Dugundji, J., "Some Dynamic Problems of Rotating Windmill Systems," *Advances in Engineering Science, Proceedings of the Thirteenth Annual Meeting of the Society of Engineering Science*, NASA CP-2001, Vol. 2, 1976, pp. 439-447.

[8] Linscott, B. S., Glasgow, J., Anderson, W. D., and Donham, R. E., "Experimental Data and Theoretical Analysis of an Operating 100 kW Wind Turbine," presented at the Twelfth Intersociety Energy Conversion Conference, Washington, D.C., Aug.-Sept. 1977.

[9] Anderson, W. D., Conner, F., Kretsinger, P., and Reasor, J. S., "Rexor Rotorcraft Simulation Model," USAAMRDL-TR-76-28A-28C, I: Engineering Documentation, II: Computer Implementation, III: User's Manual, July 1976.

[10] Hoffman, J. A., "Coupled Dynamics Analysis of Wind Energy Systems," NASA CR-135152, Feb. 1977.

[11] Warmbrodt, W., "Aeroelastic Response and Stability of a Coupled Rotor/Support System with Application to Large Horizontal Axis Wind Turbines," Ph.D. Thesis, Mechanics and Structures Dept. School of Engineering and Applied Science, University of California, Los Angeles, Calif., 1978; also available as UCLA-ENG-7881, Aug. 1978.

[12] Warmbrodt, W. and Friedman, P., "Formulation of the Aeroelastic Stability and Response Problem of Coupled Rotor/Support Systems," AIAA Paper 79-0732, *Proceedings Twentieth Structures, Structural Dynamics and Materials Conference AIAA/ASME/ASCE/AHS*, St. Louis, Mo., April 1979, pp. 39-52.

[13] Kottapalli, S.B.R., Friedmann, P. P., and Rosen, A., "Aeroelastic Stability and Response of Horizontal Axis Wind Turbine Blades," Paper C4, *Proceedings, Second International Symposium on Wind Energy Systems*, BHRA Fluid Engineering, Cranfield, Bedford, England, Vol. 1, pp. C4-49-C4-66, Oct. 1978.

[14] Kottapalli, S.B.R., Friedmann, P. P., and Rosen, A., "Aeroelastic Stability and Response of Horizontal Axis Wind Turbine Blades," School of Engineering and Applied Science Report UCLA-ENG-7880, University of California, Los Angeles, Calif., Aug. 1978.

[15] Hodges, D. H. and Ormiston, R. A., "Stability of Elastic Bending and Torsion of Uniform Cantilevered Rotor Blades in Hover with Variable Structural Coupling," NASA TN D-8192, April 1976, p. 31.

[16] Rosen, A. and Friedmann, P., "Nonlinear Equations of Equilibrium for Elastic Helicopter or Wind Turbine Blades Undergoing Moderate Deformation," School of Engineering and Applied Science Report, UCLA-ENG-7718, University of California, Los Angeles, Calif., Jan. 1977, revised, June 1977; also available as NASA CR-159478, Dec. 1978.

[17] Rosen, A. and Friedmann, P., "The Nonlinear Behavior of Elastic Slender Straight Beams Undergoing Small Strains and Moderate Rotations," *ASME Journal of Applied Mechanics*, Vol. 46, March 1979, pp. 161-168.

[18] Houbolt, J. C. and Brooks, C. W., "Differential Equations for Combined Flapwise Bending, Chordwise Bending and Torsion of Twisted Nonuniform Rotor Blades," NACA Rept. 1346, 1958.

[19] Rosen, A., "The Effect of Initial Twist on the Torsional Rigidity of Beams—Another Point of View," Technion-Israel Institute of Technology, Dept. of Aeronautical Engineering Rept., TAE No. 360, April 1978.

[20] Hodges, D. H., "Torsion of Pretwisted Beams Due to Axial Loading," submitted to the *Journal of Applied Mechanics*.

[21] Meirovitch, L., *Methods of Analytical Dynamics*, McGraw-Hill Book Co., Inc., New York, 1970.

[22] Cherritt, A. W. and Gaidelis, J. A., "100-kW Metal Wind Turbine Blade Basic Data, Loads, and Stress Analysis," NASA CR-134956, June 1975.

[23] Glasgow, J. C. and Linscott, B. S., "Early Operation Experience on the ERDA/NASA 100 kW Wind Turbine," NASA TM-71601, Sept. 1976.

[24] Shamie, J. and Friedmann, P., "Effect of Moderate Deflections on the Aeroelastic Stability of a Rotor Blade in Forward Flight," Paper 24, Third European Rotorcraft and Powered Lift Aircraft Forum, Aix-en-Provence, France, Sept. 1977.

[25] Urabe, M., "Galerkin's Procedure for Nonlinear Periodic Systems," *Archive for Rational Mechanics and Analysis*, Vol. 20, 1965, pp. 120-152.

[26] Hsu, C. S. and Cheng, W. H., "Steady-State Response of a Dynamical System Under Combined Parametric and Forcing Excitations," Paper 73-WA/APM-10, *Transactions of the ASME, Journal of Applied Mechanics*, 1973.

[27] Friedmann, P., Hammond, C. E., and Woo, T., "Efficient Numerical Treatment of Periodic Systems with Application to Stability Problems," *International Journal of Numerical Methods in Engineering*, 1977, pp. 1117-1136.

[28] Chamis, C. S. and Sullivan, R. L., "Free Vibrations of the ERDA-NASA 100 kW Wind Turbine," NASA TM X-71879, 1976.

[29] Spera, D. A., "Comparison of Computer Codes for Calculating Dynamic Loads in Wind Turbines," DOE/NASA/1028-78/16, NASA TM-73773, presented at the Third Biennial Conference and Workshop on Wind Energy Conversion Systems, Washington, D.C., Sept. 1977.